

# Three-mode entanglement by interlinked nonlinear interactions in optical $\chi^{(2)}$ media

**Alessandro Ferraro, Matteo G. A. Paris**

*Dipartimento di Fisica and Unità INFN, Università di Milano, Italy*

**Maria Bondani**

*INFN, Unità di Como, Italy*

**Alessia Allevi, Emiliano Puddu, Alessandra Andreoni**

*INFN, Unità di Como, Italy and  
Dipartimento di Fisica e Matematica,  
Università dell'Insubria, Como, Italy*

## Abstract

We address the generation of fully inseparable three-mode entangled states of radiation by interlinked nonlinear interactions in  $\chi^{(2)}$  media. We show how three-mode entanglement can be used to realize symmetric and asymmetric telecloning machines, which achieve optimal fidelity for coherent states. An experimental implementation involving a single nonlinear crystal where the two interactions take place simultaneously is suggested. Preliminary experimental results showing the feasibility and the effectiveness of the interaction scheme with seeded crystal are also presented.

© 2018 Optical Society of America

*OCIS codes:* 190.4970, 270.1670, 999.9999 entangled states of light.

## 1. Introduction

The successful demonstration of continuous variable (CV) quantum teleportation<sup>1,2,3</sup> and dense coding<sup>4</sup> opened new perspectives to quantum information technology based on Gaussian states of light. Besides having been recognized as the essential resource for teleportation<sup>1</sup> and dense coding<sup>5</sup>, the entanglement between two modes of light has been proved as a valuable resource also for cryptography<sup>6,7</sup>, improvement of optical resolution<sup>8</sup>, spectroscopy<sup>9</sup>, interferometry<sup>10</sup>, state engineering<sup>11</sup>, and tomography of states and operations<sup>12,13</sup>.

These achievements stimulated a novel interest in the generation and application of multipartite entanglement<sup>14,15,16,17</sup>, which has already received attention in the domain of discrete variables. Multipartite CV entanglement has been proposed to realize cloning at distance (telecloning)<sup>18,19</sup>, and to improve discrimination of quantum operations<sup>20</sup>. The separability properties of CV tripartite Gaussian states have been analyzed in<sup>21</sup>, where they have been classified into five different classes according to positivity of the three partial transposes that can be constructed. Moreover, it has been pointed out that genuine applications of three-mode entanglement requires fully inseparable tripartite entangled states<sup>22</sup>, *i.e.* states that are inseparable with respect to any grouping of the modes.

Experimental schemes to generate multimode entangled states have been already suggested and demonstrated. The first example, although no specific analysis was made on the entanglement properties (besides verification of teleportation), is provided by the original teleportation experiments of Ref.<sup>1</sup> where one party of a twin-beam (TWB) was mixed with a coherent state. A similar scheme, where one party of a TWB is mixed with the vacuum<sup>15</sup> has been demonstrated, and applied to controlled dense coding. More recently, a fully inseparable three-mode entangled state has been generated and verified<sup>16</sup> by mixing three independent squeezed vacuum states in a network of beam splitters. In addition, a four-mode entangled state to realize entanglement swapping with pulsed beams have been generated<sup>23</sup>.

All the above schemes are based on parametric sources, either of single-mode squeezing or of two-mode entanglement *i.e.* TWB, with multipartite entanglement resulting from further interactions in linear optical elements (*e.g.* beam splitters). In this paper, we focus on a scheme involving a single nonlinear crystal, in which the three-mode entangled state is produced by two type I, non-collinearly phase-matched interlinked bilinear interactions that simultaneously couple the three modes<sup>24</sup>. A similar interaction scheme, though

realized in type II collinear phase-matching conditions, is described in Ref.<sup>25</sup>. Compared to this work, our choice of non-collinear phase-matching provides remarkable flexibility to our experimental setup, whereas the choice of type I interaction prevents the generation of additional parties. Moreover, we avoid the losses brought about by the mode-matching in multiple beam splitters in that we achieve the three-partite entanglement as soon as we find the configuration that fulfills the phase-matching condition for both interactions.

The paper is structured as follows. In Section 2 we describe the generation of three-mode entanglement in a single nonlinear crystal where two interlinked bilinear interactions take place simultaneously. We obtain the explicit form in the Fock basis of the outgoing three-mode entangled state, and also address the characterization of entanglement. In Sections 3 and 4 we show how the three-mode entangled state obtained in our scheme, either for initial vacuum state or by seeding the crystal, can be used to build symmetric and asymmetric telecloning machines that achieve optimal fidelity for coherent states. In Section 5 we show how three-mode entanglement may be used for conditional generation of two-mode entanglement, in particular of TWB state. The scheme is of course less efficient than direct generation of TWB in a parametric amplifier, but it may be of interest in applications where *entanglement on-demand* is required. In Section 6, we discuss the experimental implementation of our generation scheme. We show the feasibility of experiments in the case of interaction with seeded crystal and report preliminary experimental results. Section 7 closes the paper with some concluding remarks.

## 2. Generation of three-mode entanglement

The interaction Hamiltonian we are going to consider is given by

$$H_{int} = \gamma_1 a_1^\dagger a_3^\dagger + \gamma_2 a_2^\dagger a_3 + h.c. . \quad (1)$$

$H_{int}$  describes two interlinked bilinear interactions taking place among three modes of the radiation field. It can be realized in  $\chi^{(2)}$  media by a suitable configuration which will be discussed in Section 6. The effective coupling constants  $\gamma_j$ ,  $j = 1, 2$ , of the two parametric processes are proportional to the nonlinear susceptibilities and the pump intensities. The Hamiltonian in Eq. (1) has been firstly studied in<sup>26</sup>, though not for the generation of entanglement. The Hamiltonian admits the following constant of motion

$$\Delta(t) \equiv N_1(t) - N_2(t) - N_3(t) \equiv \Delta(0) , \quad (2)$$

where  $N_j(t) = \langle a_j^\dagger(t)a(t) \rangle$  represent the average number of photons in the  $j$ -th mode. If we take the vacuum  $|\mathbf{0}\rangle \equiv |0\rangle_1 \otimes |0\rangle_2 \otimes |0\rangle_3$  as the initial state we have  $\Delta = 0$  *i.e.*  $N_1(t) = N_2(t) + N_3(t) \forall t$ . The expressions for  $N_j(t)$  can be obtained by the Heisenberg evolution of the field operators, which read as follows

$$\begin{aligned} a_1^\dagger(t) &= f_1 a_1^\dagger(0) + f_2 a_2(0) + f_3 a_3(0) \\ a_2(t) &= g_1 a_1^\dagger(0) + g_2 a_2(0) + g_3 a_3(0) \\ a_3(t) &= h_1 a_1^\dagger(0) + h_2 a_2(0) + h_3 a_3(0) . \end{aligned} \quad (3)$$

The explicit expressions of the coefficients  $f_j$ ,  $g_j$  and  $h_j$ ,  $j = 1, 2, 3$ , are obtained in appendix A; we omit the time dependence for brevity. By introducing  $\Omega = \sqrt{|\gamma_2|^2 - |\gamma_1|^2}$  we have

$$\begin{aligned} N_1 &= N_2 + N_3 , \\ N_2 &= \frac{|\gamma_1|^2 |\gamma_2|^2}{\Omega^4} [\cos \Omega t - 1]^2 , \\ N_3 &= \frac{|\gamma_1|^2}{\Omega^2} \sin^2(\Omega t) . \end{aligned} \quad (4)$$

The evolved state reads as follows<sup>27</sup>

$$|\mathbf{T}_0\rangle = U_t |\mathbf{0}\rangle = \frac{1}{\sqrt{1+N_1}} \sum_{pq} \left( \frac{N_2}{1+N_1} \right)^{p/2} \left( \frac{N_3}{1+N_1} \right)^{q/2} \sqrt{\frac{(p+q)!}{p!q!}} |p+q, p, q\rangle , \quad (5)$$

where  $U_t = \exp(-iH_{int}t)$  is the evolution operator, and we have already used the conservation law. The state in Eq. (5) is Gaussian, as it can be easily demonstrated by evaluating the characteristic function

$$\begin{aligned} \chi(\lambda_1, \lambda_2, \lambda_3) &= \text{Tr} [|\mathbf{T}_0\rangle \langle \mathbf{T}_0| D_1(\lambda_1) \otimes D_2(\lambda_2) \otimes D_3(\lambda_3)] \\ &= \langle \mathbf{0}| U_t^\dagger D_1(\lambda_1) \otimes D_2(\lambda_2) \otimes D_3(\lambda_3) U_t |\mathbf{0}\rangle \\ &= \exp \left[ -\frac{1}{2} (|\lambda'_1|^2 + |\lambda'_2|^2 + |\lambda'_3|^2) \right] , \end{aligned} \quad (6)$$

where  $\lambda_j$  are complex numbers,  $D_j(\lambda_j) = \exp(\lambda_j a_j^\dagger - \bar{\lambda}_j a_j)$  is a displacement operator for the  $j$ -th mode, and the primed quantities are obtained by using the Heisenberg evolution of the modes in Eq.s (3). In formulas

$$\begin{aligned} \lambda'_1 &= f_1 \lambda_1 - g_1 \bar{\lambda}_2 - h_1 \bar{\lambda}_3 \\ \lambda'_2 &= -\bar{f}_2 \lambda_1 + g_2 \lambda_2 + \bar{h}_2 \lambda_3 \\ \lambda'_3 &= -\bar{f}_3 \lambda_1 + \bar{g}_3 \lambda_2 + h_3 \lambda_3 . \end{aligned} \quad (7)$$

Following Ref.<sup>21</sup>, the characteristic function can be rewritten as

$$\chi(\lambda_1, \lambda_2, \lambda_3) = \exp \left[ -\frac{1}{4} \mathbf{x}^T \mathbf{C} \mathbf{x} \right], \quad (8)$$

where  $\mathbf{x}^T = (x_1, x_2, x_3, p_1, p_2, p_3)$ ,  $(\dots)^T$  denotes transposition,  $\lambda_j = 2^{-1/2}(p_j - ix_j)$ ,  $j = 1, 2, 3$ , and  $\mathbf{C}$  denotes the covariance matrix of the Gaussian state, whose explicit expression can be easily reconstructed from Eq.s (7). The covariance matrix determines the entanglement properties of  $|\mathbf{T}_0\rangle$ . In fact, since  $|\mathbf{T}_0\rangle$  is Gaussian the positivity of the partial transpose is a necessary and sufficient condition for separability<sup>21</sup>, which, in turn, is determined by the positivity of the matrices  $\Gamma_j = \Lambda_j \mathbf{C} \Lambda_j - i\mathbf{J}$  where  $\Lambda_1 = \text{Diag}(1, 1, 1, -1, 1, 1)$ ,  $\Lambda_2 = \text{Diag}(1, 1, 1, 1, -1, 1)$ ,  $\Lambda_3 = \text{Diag}(1, 1, 1, 1, 1, -1)$  and  $\mathbf{J}$  is the symplectic block matrix

$$\begin{pmatrix} 0 & -\mathbf{I} \\ \mathbf{I} & 0 \end{pmatrix},$$

$\mathbf{I}$  being the  $3 \times 3$  identity matrix. A numerical evaluation of the eigenvalues of  $\Gamma_j$  shows that they are nonpositive matrices  $\forall j$ . Correspondingly, the state in Eq. (5) is fully inseparable *i.e.* not separable for any grouping of the modes. Notice that the success of a true tripartite quantum protocol, as the telecloning scheme described in the following sections, is a sufficient criterion for the full inseparability of the state  $|\mathbf{T}_0\rangle$ <sup>22</sup>.

### 3. Telecloning of coherent states

Here we show how the three-mode entangled state described in the previous section can be used to achieve telecloning<sup>18</sup> of coherent states<sup>19</sup>, that is to produce two clones *at distance* of a given input radiation mode prepared in a coherent state. Depending on the values of the coupling constants of the Hamiltonian (1) the two clones can either be equal one to each other or be different. In other words, the scheme is suitable to realize both symmetric and asymmetric cloning machines<sup>28</sup>. This option can eventually be useful to fit the purpose of the clones production in order to distribute the quantum information contained in the input state<sup>29,30,31,32</sup>. Our scheme, which is analogous to that of Ref.<sup>19</sup> in the absence of an amplification process for the signal, is applied to the telecloning of coherent states, whereas the state we use to support the teleportation is the three-mode entangled state of Eq. (5). For the symmetric case we obtain an optimal cloning machine, achieving the maximum value of fidelity allowed in a continuous variable cloning process ( $F = 2/3$ )<sup>30,31,32</sup>. In the case of the asymmetric cloning a range of coupling parameters can be found that allows the fidelity

of one clone to be greater than  $2/3$ , maintaining the fidelity of the other greater than  $1/2$ , i.e. the maximum value reachable in a classical communication scheme.

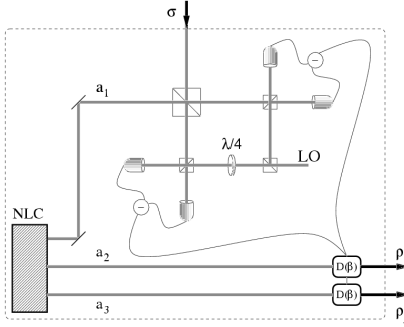


Fig. 1. Schematic diagram of the telecloning scheme. After the preparation of the state  $|\mathbf{T}_0\rangle$  by bilinear interactions in a nonlinear crystal (NLC), a conditional measurement is made on the mode  $a_1$ , which corresponds to the joint measurement of the sum- and difference-quadratures on two modes: mode  $a_1$  itself and another reference mode  $b$ , which is excited in a coherent state  $\sigma$ , to be teleported and cloned. The result of the measurement is classically sent to the parties who want to prepare approximate clones, where suitable displacement operations (see text) are performed.

A schematic diagram of our scheme is depicted in Fig. 1. After the preparation of the state  $|\mathbf{T}_0\rangle$  a conditional measurement is made on the mode  $a_1$ , which corresponds to the joint measurement of the sum- and difference-quadratures on two modes: mode  $a_1$  and another reference mode  $b$ , whose state is to be teleported and cloned. The measurement can be described as the following  $\sigma$ -dependent POVM acting on the mode  $a_1$

$$\Pi(\beta) = \frac{1}{\pi} D(\beta) \sigma^T D^\dagger(\beta), \quad (9)$$

where  $D(\beta)$ ,  $\beta \in \mathbb{C}$ , is the displacement operator, and  $\sigma$  is the preparation of  $b$ , i.e. the state to be teleported and cloned.

The probability distribution of the outcomes is given by

$$\begin{aligned} P(\beta) &= \text{Tr}_{123} [|\mathbf{T}_0\rangle\langle\mathbf{T}_0| \Pi(\beta) \otimes \mathbf{I}_2 \otimes \mathbf{I}_3] \\ &= \frac{1}{\pi(1+N_1)} \sum_{pq} \frac{N_2^p N_3^q}{(1+N_1)^{p+q}} \frac{(p+q)!}{p!q!} \langle p+q | D(\beta) \sigma^T D^\dagger(\beta) | p+q \rangle. \end{aligned} \quad (10)$$

The conditional state of the mode  $a_2$  and  $a_3$  after the outcome  $\beta$  is given by

$$\varrho_\beta = \frac{1}{P(\beta)} \text{Tr}_1 [|\mathbf{T}_0\rangle\langle\mathbf{T}_0| \Pi(\beta) \otimes \mathbf{I}_2 \otimes \mathbf{I}_3]$$

$$\begin{aligned}
&= \frac{1}{P(\beta)} \frac{1}{\pi(1+N_1)} \sum_{pqkl} \frac{N_2^{(p+k)/2} N_3^{(q+l)/2}}{(1+N_1)^{(p+q+k+l)/2}} \sqrt{\frac{(p+q)!(k+l)!}{p!q!k!l!}} \\
&\times \langle k+l | D(\beta) \sigma^T D^\dagger(\beta) | p+q \rangle | p, q \rangle \langle k, l | .
\end{aligned} \tag{11}$$

After the measurement the conditional state may be transformed by a further unitary operation, depending on the outcome of the measurement. In our case, this is a two-mode product displacement  $U_\beta = D^T(\beta) \otimes D^T(\beta)$  where the amplitude  $\beta$  is equal to the results of the measurement. This is a local transformation which generalizes to two modes the procedure already used in the original CV  $1 \rightarrow 1$  teleportation protocol. The overall state of the two modes is obtained by averaging over the possible outcomes

$$\varrho_{23} = \int_{\mathbb{C}} d^2\beta P(\beta) \tau_\beta .$$

where  $\tau_\beta = U_\beta \varrho_\beta U_\beta^\dagger$ .

If  $b$  is excited in a coherent state  $\sigma = |z\rangle\langle z|$  the probability of the outcomes is given by

$$P_z(\beta) = \frac{1}{\pi(1+N_1)} \exp \left\{ -\frac{|\beta + \bar{z}|^2}{1+N_1} \right\} . \tag{12}$$

Moreover, since the POVM is pure also the conditional state is pure. We have  $\varrho_\beta = |\psi_\beta\rangle\rangle\langle\langle\psi_\beta|$  with

$$|\psi_\beta\rangle\rangle = |\delta_{2\beta}\rangle_2 \otimes |\delta_{3\beta}\rangle_3 , \tag{13}$$

*i.e.* the product of two independent coherent states. The amplitudes are given by

$$\delta_{2\beta} = (z + \bar{\beta})\kappa_2 \quad \delta_{3\beta} = (z + \bar{\beta})\kappa_3 ,$$

where the quantities  $\kappa_j$ ,  $j = 2, 3$  are given by

$$\kappa_j = \sqrt{\frac{N_j}{1+N_1}} . \tag{14}$$

Correspondingly, we have  $\tau_\beta = U_\beta |\psi_\beta\rangle\rangle\langle\langle\psi_\beta| U_\beta^\dagger$  with

$$U_\beta |\psi_\beta\rangle\rangle = |z\kappa_2 + \bar{\beta}(\kappa_2 - 1)\rangle \otimes |z\kappa_3 + \bar{\beta}(\kappa_3 - 1)\rangle . \tag{15}$$

The partial traces  $\varrho_2 = \text{Tr}_3[\varrho_{23}]$  and  $\varrho_3 = \text{Tr}_2[\varrho_{23}]$  read as follows

$$\varrho_j = \int_{\mathbb{C}} d^2\beta P_z(\beta) |z\kappa_j + \bar{\beta}(\kappa_j - 1)\rangle\langle z\kappa_j + \bar{\beta}(\kappa_j - 1)| . \tag{16}$$

We see from the teleported states in Eq. (16) that it is possible to engineer a symmetric cloning protocol if  $N_2 = N_3 = N$ , otherwise we have an asymmetric cloning machine. Consider first the symmetric case. According to Eq.s (4) the condition  $N_2 = N_3 = N$  holds when

$$\cos \Omega t = \frac{|\gamma_1|^2}{2|\gamma_2|^2 - |\gamma_1|^2} \quad (17)$$

from which it follows that

$$N = \frac{4|\gamma_1|^2|\gamma_2|^2}{(2|\gamma_2|^2 - |\gamma_1|^2)^2}. \quad (18)$$

Since  $|\langle \beta' | \beta'' \rangle|^2 = \exp\{-|\beta' - \beta''|^2\}$ , the fidelity of the clones is given by

$$\begin{aligned} F = \langle z | \varrho_j | z \rangle &= \int_{\mathbb{C}} \frac{d^2\beta}{\pi(2N+1)} \exp\left\{-\frac{|z + \bar{\beta}|^2}{2N+1}\right\} \exp\{-|z + \bar{\beta}|^2(\kappa - 1)^2\} \\ &= \frac{1}{2 + 3N - 2\sqrt{N(2N+1)}}. \end{aligned} \quad (19)$$

As we expect from a proper cloning machine, the fidelity is independent of the amplitude of the initial signal and for  $0 < N < 4$  it is larger than the classical limit  $F = 1/2$ . Notice that the transformation  $U_\beta$  performed after the conditional measurement, is the only one assuring that the output fidelity is independent of the amplitude of the initial state. In Fig. 2 the behavior of the fidelity versus the average photon number  $N$  is shown in the relevant regime. We can see that the fidelity reaches its maximum  $F = 2/3$  for  $N = 1/2$  which means, according to Eq. (18), that the physical system allows an optimal cloning when its coupling constants are chosen so that  $|\gamma_1/\gamma_2| = \sqrt{6 - \sqrt{32}} \simeq 0.586$ . Let us now consider the asymmetric case. For  $N_2 \neq N_3$  the fidelities  $F_j = \langle z | \varrho_j | z \rangle$  of the two clones (16) are given by

$$F_2 = \frac{1}{2 + N_3 + 2N_2 - 2\sqrt{N_2(N_2 + N_3 + 1)}} \quad (20)$$

$$F_3 = \frac{1}{2 + N_2 + 2N_3 - 2\sqrt{N_3(N_2 + N_3 + 1)}}. \quad (21)$$

A question arises whether it is possible to tune the coupling constants so as to obtain a fidelity larger than the bound  $F = 2/3$  for one of the clones, say  $\varrho_2$ , while accepting a decreased fidelity for the other clone. Indeed, for example, if we impose  $F_3 = 1/2$ , *i.e.* the minimum value to assure the genuine quantum nature of the telecloning protocol, then we should choose  $N_3 = \frac{1}{4}N_2^2$ . In this case the maximum value for  $F_2$  is given by  $F_{2max} = 4/5$ ,



which occurs for  $N_2 = 1$ . More generally, by substituting Eq. (21) in Eq. (20) and maximizing  $F_2$  with respect to  $N_2$  keeping  $F_3$  fixed, we obtain that for  $N_2 = 1/F_3 - 1$  and  $N_3 = 1/4(1/F_3 - 1)^{-1}$  we have

$$F_2 = 4 \frac{(1 - F_3)}{(4 - 3F_3)},$$

which shows that  $F_2$  is a decreasing function of  $F_3$  and that  $2/3 < F_2 < 4/5$  for  $1/2 < F_3 < 2/3$ . Notice that the sum of the two fidelities  $F_2 + F_3 = 1 + 3/4F_2F_3$  is not constant, being maximum in the symmetric case  $F_2 = F_3 = 2/3$ . Notice also that the roles of  $\varrho_2$  and  $\varrho_3$  are interchangeable in the considerations.

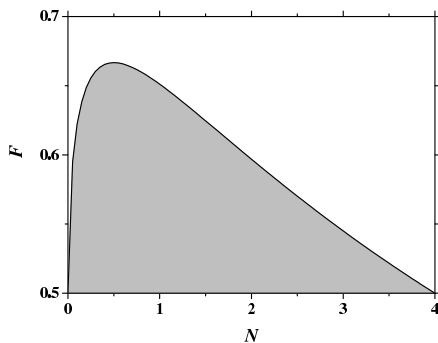


Fig. 2. Fidelity of symmetric clones versus the average (equal) photon number  $N$  of modes  $a_2$  and  $a_3$ .

#### 4. Telecloning with seeded crystal

In order to confirm the feasibility of the telecloning scheme presented in the previous section we now show that the same protocol can be implemented also when the state that supports teleportation is generated by Hamiltonian (1) starting from a coherent state in one of the modes, rather than from the vacuum. This may be of interest from the experimental point of view, since seeding a crystal with a coherent beam is a useful technique to align the setup, and allows the verification of the classical evolution of the interacting fields [see Section 6].

The analysis of the scheme is analogue to that of the previous Section, however starting from the initial state  $|\alpha, 0, 0\rangle$  instead of the vacuum. The explicit expression of the evolved state  $|\mathbf{T}_\alpha\rangle$  is derived in appendix B. Notice that the conservation law (2) implies that the populations for seeded crystal  $N_{j\alpha} = \langle \mathbf{T}_\alpha | a_j^\dagger a_j | \mathbf{T}_\alpha \rangle$  satisfies the relation  $N_{1\alpha} - N_{2\alpha} - N_{3\alpha} = |\alpha|^2$ . We refer the reader to appendix B for the explicit expressions of  $N_{j\alpha}$  and for their connections to the populations  $N_j$  for vacuum input.

A compact expression for the evolved state is the following

$$|\mathbf{T}_\alpha\rangle = D_1(\alpha f_1(-t)) \otimes D_2(\overline{-\alpha f_2(-t)}) \otimes D_3(\overline{-\alpha f_3(-t)}) |\mathbf{T}_0\rangle, \quad (22)$$

where the  $f_j(t)$ ,  $j = 1, 2, 3$  are given in appendix A. Expression (22) can be easily derived by using the Heisenberg equation of motion for the field-mode  $a_1(t)$  (see Eq.s (3)). The telecloning process proceed as in the previous Section, with calculations performed using the shifted Fock basis  $|\psi_n\rangle_1 \equiv D_1(\alpha f_1)|n\rangle_1$ , and  $|\psi_n\rangle_j \equiv D_j(\overline{-\alpha f_j})|n\rangle_j$ ,  $j = 2, 3$ . If the reference mode  $b$  is excited in a pure coherent state  $\sigma = |z\rangle\langle z|$ , then, as in Section 3, the conditional state is pure  $\varrho_\beta = |\psi_\beta\rangle\rangle\langle\langle\psi_\beta|$  with

$$|\psi_\beta\rangle\rangle = |\zeta_{2\beta}\rangle_2 \otimes |\zeta_{3\beta}\rangle_3, \quad (23)$$

*i.e.* the product of two independent coherent states. The amplitudes are given by

$$\zeta_{2\beta} = (z + \bar{\beta} - \overline{\alpha f_1})\kappa_2 - \overline{\alpha f_2} \quad \zeta_{3\beta} = (z + \bar{\beta} - \overline{\alpha f_1})\kappa_3 - \overline{\alpha f_3},$$

where the quantities  $\kappa_j$ ,  $j = 2, 3$  are given by Eq. (14). The unitary transformation on  $a_2$  and  $a_3$  that completes the telecloning is now given by

$$U_\beta = D_2^\dagger(\bar{\beta} - \kappa_2\overline{\alpha f_1} - \overline{\alpha f_2}) \otimes D_3^\dagger(\bar{\beta} - \kappa_3\overline{\alpha f_1} - \overline{\alpha f_3}). \quad (24)$$

In fact, the output conditional state coincides with that of Eq. (15), so that the partial traces are identical to those given in Eq. (16). For  $N_2 = N_3 = N$  we obtain symmetric clones with the same fidelity as in Section 3. Moreover conditions (17) and (18) still hold. Notice that also the protocol for asymmetric cloning can be straightforwardly extended to the present seeded scheme.

## 5. Conditional generation of two-mode entanglement

Another application of the three-mode entangled state of Eq. (5) is the conditional generation of a two-mode entangled state of radiation by on-off photodetection on one of the modes of state  $|\mathbf{T}_0\rangle$ . Indeed, it is possible to produce a robust two-mode entangled state that approaches a TWB for unit quantum efficiency  $\eta$  of the photodetector. In the following we evaluate some properties of the conditional state when  $\eta \neq 1$  in order to quantify its closeness to an ideal TWB. Notice that, due to the well known properties of TWB, this scheme also provides a valid check of the whole apparatus from an experimental viewpoint.

Let us consider the situation in which a mode of the state  $|\mathbf{T}_0\rangle$ , say the third mode, is revealed by an on-off photodetector. The probability operator measure (POVM) is two-valued  $\{\Pi_0, \Pi_1\}$ ,  $\Pi_0 + \Pi_1 = \mathbf{I}$ , with the element associated to the "no photons" result given by

$$\Pi_0 = \mathbf{I}_1 \otimes \mathbf{I}_2 \otimes \sum_n (1 - \eta)^n |n\rangle_{33} \langle n|. \quad (25)$$

The probability of the outcome is given by

$$\begin{aligned} P_0 &= \text{Tr}_{123} [|\mathbf{T}_0\rangle \langle \mathbf{T}_0| \Pi_0] \\ &= \frac{1}{1 + N_1} \sum_{m,n} \left( \frac{N_2}{1 + N_1} \right)^n \left( \frac{N_3(1 - \eta)}{1 + N_1} \right)^m \frac{(n + m)!}{n!m!} \\ &= (1 + \eta N_3)^{-1}, \end{aligned} \quad (26)$$

while the conditional output state  $\varrho_0 = \frac{1}{P_0} \text{Tr}_3 [|\mathbf{T}_0\rangle \langle \mathbf{T}_0| \Pi_0]$  reads as follows

$$\varrho_0 = \frac{1 + \eta N_3}{1 + N_1} \sum_{m,n,n'} \left( \frac{N_2}{1 + N_1} \right)^{\frac{n+n'}{2}} \left( \frac{N_3(1 - \eta)}{1 + N_1} \right)^m \frac{1}{m!} \sqrt{\frac{(n + m)!(n' + m)!}{n!n'!}} |n + m, n\rangle \langle n' + m, n'| \quad (27)$$

Remind that  $N_1 = N_2 + N_3$ . If  $\eta = 1$  this state reduces to the following TWB

$$|\psi_0\rangle = \sqrt{\frac{1 + N_3}{1 + N_1}} \sum_n \left( \frac{N_2}{1 + N_1} \right)^{\frac{n}{2}} |n, n\rangle. \quad (28)$$

When the efficiency of the detector is not unitary a question arises on how to quantify the closeness of  $\varrho_0$  to the ideal state  $|\psi_0\rangle$ . From an operational point of view, we can evaluate the photon number correlation between the first and second mode, which is defined as

$$\zeta_{12} = \frac{\langle (n_1 - n_2)^2 \rangle - (\langle n_1 \rangle - \langle n_2 \rangle)^2}{\langle n_1 \rangle + \langle n_2 \rangle}, \quad (29)$$

and is zero in case of TWB. After straightforward calculations we arrive at

$$\zeta_{12} = \frac{N_3(1 - \eta)(1 + N_3)}{(1 + \eta N_3)[2N_2 + N_3(1 - \eta)]}, \quad (30)$$

which, for any given value of the quantum efficiency  $\eta$ , is a decreasing function of  $N_2$  and an increasing function of  $N_3$ . A global quantity to characterize the state in Eq. (27) is the fidelity with a reference TWB state. The natural choice for the reference is the TWB  $|\psi_0\rangle$ , according to the following argument. At first we calculate the fidelity between state (27)

and a generic TWB of parameter  $\xi$  *i.e.*  $|\xi\rangle = \sqrt{1-\xi^2} \sum \xi^n |n, n\rangle$ , we have

$$\begin{aligned}
F(\eta, \xi) &= \langle \xi | \rho_0 | \xi \rangle = (1 - \xi^2) \frac{1 + \eta N_3}{1 + N_1} \\
&\times \sum_{m, n, n', p, q} \xi^{p+q} \left( \frac{N_2}{1 + N_1} \right)^{\frac{n+n'}{2}} \left( \frac{N_3(1-\eta)}{1 + N_1} \right)^m \frac{1}{m!} \sqrt{\frac{(n+m)!(n'+m)!}{n!n'!}} \delta_n^p \delta_{n'}^q \delta_0^m \\
&= \frac{1 + \eta N_3}{1 + N_1} \frac{1 - \xi^2}{\left(1 - \xi \sqrt{N_2/(1 + N_1)}\right)^2}. \tag{31}
\end{aligned}$$

Then, we look for the parameter  $\xi$  that maximizes the fidelity. Expression (31) shows that the value of  $\xi$  maximizing the fidelity is, independently on  $\eta$ ,  $\xi = \sqrt{N_2/(1 + N_1)}$ . By substituting in Eq. (31) we arrive at

$$F(\eta) = \frac{1 + \eta N_3}{1 + N_3}. \tag{32}$$

Therefore, the maximum fidelity is obtained for  $\eta = 1$  and the correct reference state is the TWB  $|\psi_0\rangle$ . In conclusion, the state generated through conditional on/off photodetection on the third mode of  $|\mathbf{T}_0\rangle$  is a robust two-mode entangled state with a fidelity to a TWB given by (32). Notice that  $\eta < F(\eta) < 1$  for any choice of  $N_3$ . The same analysis is valid for a conditional measurement performed on mode  $a_2$ , in which case we obtain an entangled state of modes  $a_1$  and  $a_3$  [in this case the role of  $N_2$  and  $N_3$  should be exchanged in Eq.s (30), (31), and (32)]. On the other hand, we notice that a conditional photodetection on mode  $a_1$  does not lead to an entangled state of modes  $a_2$  and  $a_3$ .

## 6. The optical scheme

An experimental implementation of the scheme proposed in this paper can be obtained by using a single nonlinear crystal in which the two interactions described by Hamiltonian (1) take place simultaneously. The interactions correspond to two phase-matched second-order nonlinear processes in which five fields interact and two of them do not evolve (parametric approximation). Among the five fields  $a_j$  involved in the interactions,  $a_4$  and  $a_5$  will be the non-evolving pump-fields.

The energy-matching and phase-matching conditions required by the interactions can be written as  $\omega_4 = \omega_1 + \omega_3$ ,  $\omega_2 = \omega_3 + \omega_5$ ,  $\mathbf{k}_4 = \mathbf{k}_1 + \mathbf{k}_3$  and  $\mathbf{k}_2 = \mathbf{k}_3 + \mathbf{k}_5$ , being  $\mathbf{k}_j$  the wave-vectors (in the medium) corresponding to  $\omega_j$ , which make angles  $\vartheta_j$  with the normal to the entrance face of the crystal. It is possible to satisfy these phase-matching conditions with a

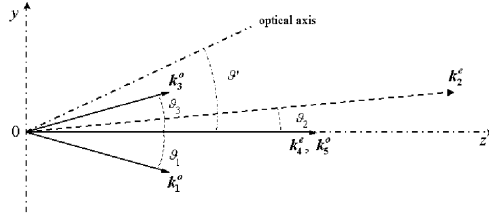


Fig. 3. Interaction scheme. The pump beams  $a_4$  and  $a_5$  are supposed to impinge on the crystal face along the normal. The values of the crystal cut angle,  $\vartheta'$ , and of the interaction angles  $\vartheta_1$ ,  $\vartheta_2$ , and  $\vartheta_3$ , are calculated to satisfy the phase-matching conditions. The wavelengths of the interacting modes are  $\lambda(\omega_1) = \lambda(\omega_3) = 1064$  nm,  $\lambda(\omega_4) = \lambda(\omega_5) = 532$  nm and  $\lambda(\omega_2) = 355$  nm.

number of different choices of frequencies and interaction angles depending on the choice of the nonlinear medium. Here we propose an experimental setup based on a  $\beta$ -BaB<sub>2</sub>O<sub>4</sub> crystal (BBO, cut angle 32 deg, cross section  $10 \times 10$  mm<sup>2</sup> and 4 mm thickness, Fujian Castech Crystals Inc., Fuzhou, China) as the nonlinear medium and the harmonics of a Q-switched amplified Nd:YAG laser (7 ns pulse duration, Quanta-Ray GCR-3-10, Spectra-Physics Inc., Mountain View, CA) as the interacting fields. We choose a compact interaction geometry in which two type I non-collinear interactions with the two pump-beams superimposed in a single beam with mixed polarization take place (see Fig. 3). With reference to Fig. 3, the wavelengths of the interacting modes are  $\lambda(\omega_1) = \lambda(\omega_3) = 1064$  nm,  $\lambda(\omega_4) = \lambda(\omega_5) = 532$  nm and  $\lambda(\omega_2) = 355$  nm. The interaction angles, calculated by supposing that the two pump beams propagate along the normal to the crystal entrance face, result to be  $\vartheta' = 37.74$  deg,  $\vartheta_1 = -\vartheta_3 = 10.6$  deg and  $\vartheta_2 = 3.5$  deg, and since the crystal we used was cut at 32 deg, it had to be rotated to allow phase matching. In order to demonstrate the feasibility of the scheme in Fig. 3, we adopted the experimental setup depicted in Fig. 4. The fundamental and second harmonic outputs of the Nd:YAG laser were sent to a harmonic separator and then each beam was collimated to a diameter suitable to illuminate the BBO crystal. The polarization of the second harmonic beam emerging from the laser is elliptic, and the two polarization components were separated through a thin-film plate polarizer ( $P_1$  in Fig. 4). On the ordinarily polarized component a  $\lambda/2$  plate was inserted to modulate the intensity of beam  $a_5$ , without affecting the intensity of the other pump,  $a_4$ . The two beams were then recombined through a second thin-film plate polarizer ( $P_2$ ) and sent to the BBO. As a

first verification of the effectiveness of the interaction described by the Hamiltonian (1), we implemented the seeded configuration discussed in Section 4 by injecting the BBO with a portion of the fundamental laser output (see Fig. 4) to realize the initial condition for field  $a_1$ .

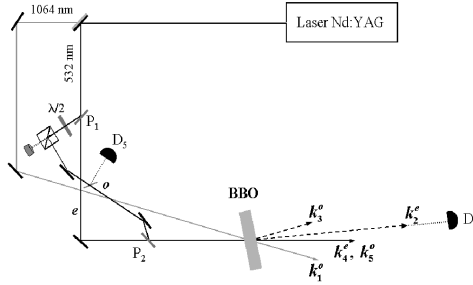


Fig. 4. Experimental setup. The fundamental and second harmonic outputs of the Nd:YAG laser are sent to a harmonic separator and then each beam is collimated to a diameter suitable to illuminate the BBO crystal. The polarization of the second harmonic beam emerging from the laser is elliptic, and the two polarization components are separated by a thin-film plate polarizer ( $P_1$ ). On the ordinarily polarized component a  $\lambda/2$  plate is inserted to modulate the intensity of beam  $a_5$ , without affecting the intensity of the other pump,  $a_4$ . The two beams then recombine at a second thin-film plate polarizer ( $P_2$ ) and are sent to the BBO.  $D_5$  and  $D_2$  are pyroelectric detectors.

As a first quantitative check, we measured the energy,  $E_2$ , of the beam generated at  $\omega_2$  as a function of the energy,  $E_5$ , of the ordinarily polarized pump-beam for fixed values of the energies of the extraordinarily polarized pump-beam,  $E_4$ , and of the seed-beam,  $E_1$ . We preliminarily measured  $E_1$  by using a pyroelectric detector (ED200, Gentec Electro-Optics Inc., Quebec, QC, Canada) which also allows checking the stability of the source. By averaging over more than 100 pulses we found a value of about 48 mJ per pulse, only 50% of which is ordinarily polarized, and thus suitable for the interaction. To measure energy  $E_4$  we inserted another pyroelectric detector (mod. ED500, Gentec) after  $P_2$ . By averaging again over more than 100 pulses we found a value of about 158 mJ per pulse. To obtain a reliable measurement of  $E_5$  we inserted, on the path of beam  $a_5$ , a cube beam splitter and a calibrated glass plate to extract a fraction of the beam. Energy  $E_5$  was varied by rotating the  $\lambda/2$  plate, and its measurement was performed with the same detector ED500 as before (see  $D_5$  in Fig. 4)). To measure the energy  $E_2$  of the output pulses we used another

pyroelectric detector (PE10, Ophir Optronics Ltd., Jerusalem, Israel, see  $D_2$  in Fig. 4)). The values of  $E_5$  and  $E_2$  were measured simultaneously as averages over the same 20 laser shots at each rotation of the  $\lambda/2$  plate. In Fig 5 we show the measured values of  $E_2$  (open circles), as a function of the measured values of  $E_5$ . We can compare the experimental results with the field evolution calculated according to the classical equations<sup>24</sup>

$$E_2 = \frac{\omega_2}{\omega_1} \frac{c_1 E_4 \cdot c_2 E_5}{(c_2 E_5 - c_1 E_4)^2} \left[ \cos \left( \sqrt{c_2 E_5 - c_1 E_4} z \right) - 1 \right]^2 E_1 \quad (33)$$

where  $c_1 = 8.3 \times 10^4 (\text{Jm}^2)^{-1}$  and  $c_2 = 2.6 \times 10^5 (\text{Jm}^2)^{-1}$  are the coupling constants that apply to the present interactions. In Fig 5 we show the values (full circles) of  $E_2$  as calculated according to Eq. (33) for the experimental values of  $E_5$ , and for fixed values  $E_1 = 24$  mJ and  $E_4 = 158$  mJ. The agreement between measured and calculated values is excellent.

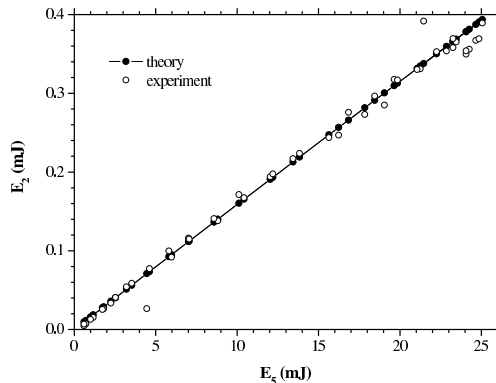


Fig. 5. Comparison of the experimental results with the field evolution calculated according to equation (33). Open circles: measured values of the energy of field  $a_2$  as a function of the measured values of the energy of pump-field  $a_5$ . Full circles: values of the energy of field  $a_2$  as calculated from the classical evolution of the interacting fields as a function of the measured values of the energy of pump-field  $a_5$ .

## 7. Conclusions and outlooks

We have suggested a scheme to generate fully inseparable three-mode entangled states of radiation based on interlinked bilinear interactions taking place in a single  $\chi^{(2)}$  nonlinear crystal. We have shown how the resulting three-mode entanglement can be used to realize symmetric and antisymmetric telecloning machines that achieve optimal fidelity for coherent states. An experimental implementation involving a BBO nonlinear crystal is suggested and the feasibility of the scheme is analyzed. Preliminary experimental results are presented:

as a first quantitative check, we measured the energy of the beam generated at  $\omega_2$  as a function of the energy of the ordinarily polarized pump, for fixed values of the energies of the extraordinarily polarized pump-beam, and of the seed-beam. The agreement between measured and calculated values is excellent.

To realize the telecloning protocol described in Section 3 we need to generate three-mode entanglement from vacuum. This should be possible by implementing the same experimental setup as in Fig. 4 with a different laser source able to deliver a higher intensity. In fact, we plan to use a mode-locked amplified Nd:YLF laser (IC-500, HIGH Q Laser Production, Hohenems, Austria) with which it is easy to achieve an intensity value of 50 GW/cm<sup>2</sup> in a collimated beam. Since such a value was enough to generate bright twin beams in a 4-mm thick BBO crystal, it should allow us to obtain the three-mode entangled state described in this paper, not only by seeding the crystal but also for initial vacuum state.

### Acknowledgment

This work has been supported by the INFN through the project PRA-2002-CLON and by MIUR through the project FIRB-RBAU014CLC. The authors thank M. Cola and N. Piovella (Università di Milano) for fruitful discussions, and F. Paleari and F. Ferri (Università dell'Insubria) for experimental support.

### References

1. A. Furusawa, J. L. Sørensen, S. L. Braunstein, C. A. Fuchs, H. J. Kimble, and E. S. Polzik, “Unconditional quantum teleportation,” *Science* **282**, 706 (1998).
2. W. P. Bowen, N. Treps, B. C. Buchler, R. Schnabel, T. C. Ralph, H. A. Bachor, T. Symul, and P. K. Lau, “Experimental investigation of continuous-variable quantum teleportation,” *Phys. Rev. A* **67**, 032302 (2003).
3. T. C. Zhang, K. W. Goh, C. W. Chon, P. Lodahl, and H. J. Kimble, “Quantum teleportation of light beams,” *Phys. Rev. A* **67**, 033802 (2003).
4. X. Li, Q. Pan, J. Jing, J. Zhang, C. Xie, and K. Peng, “Quantum dense coding exploiting a bright Einstein-Podolsky-Rosen beam,” *Phys. Rev. Lett.* **88**, 047904 (2002).
5. M. Ban, “Quantum dense coding of continuous variables in a noisy quantum channel,” *J. Opt. B* **2**, 786 (2000); T. C. Ralph, E. H. Huntington, “Unconditional continuous-variable dense coding,” *Phys. Rev A* **66** 042321 (2002).



6. Ch. Silberhorn, T. C. Ralph, N. Lütkenhaus, and G. Leuchs, “Continuous variable quantum cryptography: beating the 3dB loss limit,” *Phys. Rev. Lett.* **89**, 167901 (2002).
7. Ch. Silberhorn, N. Korolkova, and G. Leuchs, “Quantum key distribution with bright entangled beams,” *Phys. Rev. Lett.* **88**, 167902 (2002).
8. M. I. Kolobov and C. Fabre, “Quantum limits on optical resolution,” *Phys. Rev. Lett.* **85** 3789 (2000).
9. B. E. A. Saleh, B. M. Jost, H.-B. Fei, and M. C. Teich, “Entangled-photon virtual-state spectroscopy,” *Phys. Rev. Lett.* **80** 3483 (1998).
10. G. M. D’Ariano, M. G. A. Paris and P. Perinotti, “Improving quantum interferometry using entanglement,” *Phys. Rev A* **65** 062106 (2002).
11. M. G. A. Paris, M. Cola, and R. Bonifacio, “Quantum state engineering assisted by entanglement,” *Phys. Rev. A* **67**, 042104 (2003).
12. G. M. D’Ariano, and P. Lo Presti, “Quantum tomography for measuring experimentally the matrix elements of an arbitrary quantum operation,” *Phys. Rev. Lett.* **86** 4195 (2001).
13. G. M. D’Ariano, P. Lo Presti and M. G. A. Paris, “Using entanglement improves the precision of quantum measurements,” *Phys. Rev. Lett.* **87**, 270404 (2001).
14. J. Zhang, C. Xie, and K. Peng, “Controlled dense coding for continuous variables using three-particle entangled states,” *Phys. Rev. A* **66**, 032318 (2002).
15. J. Jing, J. Zhang, Y. Yan, F. Zhao, C. Xie, K. Peng, “Experimental demonstration of tripartite entanglement and controlled dense coding for continuous variables,” *Phys. Rev. Lett.* **90** 167903 (2003).
16. T. Aoki, N. Takey, H. Yonezawa, K. Wakui, T. Hiraoka, A. Furusawa, and P. van Loock, “Experimental creation of a fully inseparable tripartite continuous-variable state,” *Phys. Rev. Lett.* **91**, 080404 (2003).
17. P. van Loock and A. Furusawa, “Detecting genuine multipartite continuous-variable entanglement,” *Phys. Rev. A* **67**, 052315 (2003).
18. M. Muro, D. Jonathan, M. B. Plenio, and V. Vedral, “Quantum telecloning and multiparticle entanglement,” *Phys. Rev. A* **59**, 156 (1999);
19. P. van Loock, and S. Braunstein, “Telecloning of continuous quantum variables,” *Phys. Rev. Lett.* **87**, 247901 (2001).

20. G. M., D'Ariano, P. Lo Presti, and M. G. A. Paris, "Improved discrimination of unitary transformation by entangled probes," *J. Opt. B*, **4**, S273 (2002).
21. G. Giedke, B. Kraus, M. Lewenstein, and J. I. Cirac, "Separability properties of three-mode Gaussian states," *Phys. Rev. A* **64**, 052303 (2001).
22. P. van Loock, and S. Braunstein, "Multipartite entanglement for continuous variables: a quantum teleportation network," *Phys. Rev. Lett.* **84**, 3482 (2000).
23. O. Glöckl, S. Lorenz, C. Marquardt, J. Heersink, M. Brownnutt, C. Silberhorn, Q. Pan, P. van Loock, N. Korolkova, and G. Leuchs, "Experiment towards continuous-variable entanglement swapping: Highly correlated four-partite quantum state," *Phys. Rev. A* **68** 012319 (2003).
24. A. Allevi, A. Andreoni, M. Bondani, E. Puddu, A. Ferraro, and M. G. A. Paris, "Properties of two interlinked  $\chi^{(2)}$  interactions in non-collinear phase-matching," *Optics Lett.* **29** (2004), IN PRESS (15 Jan 04, please add the complete reference)
25. R. A. Andrews, H. Rabin, and C. L. Tang, "Coupled parametric downconversion and upconversion with simultaneous phase matching," *Phys. Rev. Lett.* **25**, 605-608 (1970).
26. M. E. Smithers, E. Y. C. Lu, "Quantum theory of coupled parametric down-conversion and up-conversion with simultaneous phase matching," *Phys. Rev. A* **10**, 1874 (1974).
27. N. Piovella, M. Cola, and R. Bonifacio, *Phys. Rev. A* **67**, "Quantum fluctuations and entanglement in the collective atomic recoil laser using a Bose-Einstein condensate," 013817 (2003).
28. S.L. Braunstein, V. Buzek, and M. Hillery, "Quantum-information distributors: Quantum network for symmetric and asymmetric cloning in arbitrary dimension and continuous limit," *Phys. Rev. A* **63**, 052313 (2001); N. J. Cerf, "Asymmetric quantum cloning in any dimension," *J. Mod. Opt.* **47**, 187 (2000).
29. N. J. Cerf, A. Ipe, X. Rottenberg, "Cloning of continuous quantum variables," *Phys. Rev. Lett.* **85**, 1754 (2000).
30. S. L. Braunstein, N. J. Cerf, S. Iblisdir, P. van Loock, and S. Massar, "Optimal cloning of coherent states with a linear amplifier and beam splitters," *Phys. Rev. Lett.* **86**, 4938 (2001).
31. J. Fiurasek, "Optical implementation of continuous-variables quantum cloning machines," *Phys. Rev. Lett.* **86**, 4942 (2001).
32. N. J. Cerf, S. Iblisdir, and G. van Assche, "Cloning and cryptography with quantum

continuous variables,” Eur. Phys. J. D **18**, 211 (2002).

### Appendix A: Heisenberg evolution of modes

In this section we calculate the dynamics generated by the Hamiltonian (1) in the Heisenberg picture. The equations of motion are given by

$$\begin{aligned}\dot{a}_1^\dagger &= i\bar{\gamma}_1 a_3 \\ \dot{a}_2 &= -i\gamma_2 a_3 \\ \dot{a}_3 &= -i\gamma_1 a_1^\dagger - i\bar{\gamma}_2 a_2 .\end{aligned}\tag{A1}$$

This system of differential equations can be Laplace transformed in the following algebraic system

$$\begin{aligned}a_1^\dagger(0) + \mu\tilde{a}_1^\dagger(\mu) &= i\bar{\gamma}_1\tilde{a}_3(\mu) \\ a_2(0) + \mu\tilde{a}_2(\mu) &= -i\gamma_2\tilde{a}_3(\mu) \\ a_3(0) + \mu\tilde{a}_3(\mu) &= -i\gamma_1\tilde{a}_1^\dagger(\mu) - i\bar{\gamma}_2\tilde{a}_2(\mu) ,\end{aligned}\tag{A2}$$

where we have defined the Laplace transform of  $a_j(t)$

$$\tilde{a}_j(\mu) \equiv \int_0^\infty dt e^{-\mu t} a_j(t) .\tag{A3}$$

The determinant of the system (A2) is

$$\Delta = \mu(\mu + \Gamma)(\mu - \Gamma) ,\tag{A4}$$

where  $\Gamma \equiv \sqrt{|\gamma_1|^2 - |\gamma_2|^2}$ , therefore its solution reads

$$\begin{aligned}\tilde{a}_1^\dagger(\mu) &= \frac{1}{\Delta} \left[ (|\gamma_2|^2 + \mu^2)a_1^\dagger(0) + \bar{\gamma}_1\bar{\gamma}_2 a_2(0) + i\bar{\gamma}_1\mu a_3(0) \right] \\ \tilde{a}_2(\mu) &= \frac{1}{\Delta} \left[ -\gamma_1\gamma_2 a_1^\dagger(0) + (\mu^2 - |\gamma_1|^2)a_2(0) - i\gamma_2\mu a_3(0) \right] \\ \tilde{a}_3(\mu) &= \frac{1}{\Delta} \left[ -i\gamma_1\mu a_1^\dagger(0) - i\mu\bar{\gamma}_2 a_2(0) + \mu^2 a_3(0) \right] .\end{aligned}\tag{A5}$$

The solution of system (A1) follows from anti-transforming Eq. (A5). We have

$$a_1^\dagger(t) = f_1 a_1^\dagger(0) + f_2 a_2(0) + f_3 a_3(0)\tag{A6}$$

$$a_2(t) = g_1 a_1^\dagger(0) + g_2 a_2(0) + g_3 a_3(0)\tag{A7}$$

$$a_3(t) = h_1 a_1^\dagger(0) + h_2 a_2(0) + h_3 a_3(0)\tag{A8}$$

where the coefficients are given by

$$f_1(t) = \frac{1}{\Omega^2} [|\gamma_1|^2 \cos \Omega t - |\gamma_2|^2] \quad (\text{A9})$$

$$f_2(t) = \frac{\overline{\gamma_1} \gamma_2}{\Omega^2} [\cos \Omega t - 1] \quad (\text{A10})$$

$$f_3(t) = i \frac{\overline{\gamma_1}}{\Omega} \sin(\Omega t) \quad (\text{A11})$$

$$g_1(t) = \frac{\gamma_1 \gamma_2}{\Omega^2} [1 - \cos \Omega t] \quad (\text{A12})$$

$$g_2(t) = \frac{1}{\Omega^2} [|\gamma_1|^2 - |\gamma_2|^2 \cos \Omega t] \quad (\text{A13})$$

$$g_3(t) = -i \frac{\gamma_2}{\Omega} \sin(\Omega t) \quad (\text{A14})$$

$$h_1(t) = -i \frac{\gamma_1}{\Omega} \sin(\Omega t) \quad (\text{A15})$$

$$h_2(t) = -i \frac{\overline{\gamma_2}}{\Omega} \sin(\Omega t) \quad (\text{A16})$$

$$h_3(t) = \cos(\Omega t) \quad (\text{A17})$$

and  $\Omega \equiv i\Gamma = \sqrt{|\gamma_2|^2 - |\gamma_1|^2}$ .

## Appendix B: Schrodinger evolution in a seeded crystal

In this appendix we derive the explicit expression of the evolved state from  $|\alpha, 0, 0\rangle$ . We can write the Hamiltonian (1) as follows:

$$H_{int} = \gamma_1 K^\dagger + \overline{\gamma_2} J + h.c. , \quad (\text{B1})$$

with the definitions  $K \equiv a_1 a_3$  and  $J \equiv a_2 a_3^\dagger$ . To calculate the evolved state we can proceed by factorizing the temporal evolution operator of the system; to this purpose we introduce the following operators

$$J_1 \equiv a_1 a_1^\dagger + a_3^\dagger a_3 , \quad J_2 \equiv a_3^\dagger a_3 - a_2^\dagger a_2 , \quad M \equiv a_1 a_2 ,$$

which form with K and J a closed algebra. Actually, the temporal evolution operator can be written in the following way:

$$\hat{U}(t) = e^{\beta_1 K^\dagger} e^{\beta_2 M^\dagger} e^{\beta_3 J^\dagger} e^{\beta_4 J_1} e^{\beta_5 J_2} e^{\beta_6 J} e^{\beta_7 K} e^{\beta_8 M} , \quad (\text{B2})$$

which allows us to calculate the evolution of a generic initial state as a function of  $\beta_i$ . In the case under investigation we obtain:

$$\begin{aligned}
\hat{U}(t)|\alpha, 0, 0\rangle &= \hat{U}(t)e^{-\frac{|\alpha|^2}{2}} \sum_n \frac{\alpha^n}{\sqrt{n!}} |n, 0, 0\rangle \\
&= e^{-\frac{|\alpha|^2}{2}} e^{\beta_1 K^\dagger} e^{\beta_2 M^\dagger} e^{\beta_3 J^\dagger} e^{\beta_4 J_1} \sum_n \frac{\alpha^n}{\sqrt{n!}} |n, 0, 0\rangle \\
&= e^{-\frac{|\alpha|^2}{2}} e^{\beta_1 K^\dagger} e^{\beta_2 M^\dagger} e^{\beta_3 J^\dagger} e^{\beta_4} \sum_n \frac{(\alpha e^{\beta_4})^n}{\sqrt{n!}} |n, 0, 0\rangle \\
&= e^{-\frac{|\alpha|^2}{2}} e^{\beta_4} e^{\beta_1 K^\dagger} \sum_{n,p} \frac{(\alpha e^{\beta_4})^n}{\sqrt{n!}} \frac{\beta_2^p}{\sqrt{p!}} \frac{\sqrt{(n+p)!}}{\sqrt{n!}} |n+p, p, 0\rangle \\
&= e^{-\frac{|\alpha|^2}{2}} e^{\beta_4} \sum_{n,p,q} \beta_1^q \beta_2^p (\alpha e^{\beta_4})^n \frac{\sqrt{(n+p+q)!}}{n! \sqrt{p!q!}} |n+p+q, p, q\rangle. \tag{B3}
\end{aligned}$$

It can be demonstrated<sup>27</sup> that

$$e^{\beta_4} = \frac{1}{\sqrt{1+N_1}}, \quad \beta_1 = \sqrt{\frac{N_3}{1+N_1}}, \quad \beta_2 = \sqrt{\frac{N_2}{1+N_1}}.$$

Moreover, for the population with initial vacuum  $N_j = \langle \mathbf{T}_0 | a_j^\dagger a_j | \mathbf{T}_0 \rangle$  and initial seed  $N_{j\alpha} = \langle \mathbf{T}_\alpha | a_j^\dagger a_j | \mathbf{T}_\alpha \rangle$  we have the relations

$$N_1 = \frac{N_{1\alpha} - |\alpha|^2}{1 + |\alpha|^2}, \quad N_2 = \frac{N_{2\alpha}}{1 + |\alpha|^2}, \quad N_3 = \frac{N_{3\alpha}}{1 + |\alpha|^2}.$$